Research Article

# Mechanism of underexcavation and practical design method for building rectification

**Junhua Xiao**[1,2] (ID) · **Jianping Sun**[1,2] · **Xin Zhang**[1,2] · **Qingxia Yue**[1,2]

## Abstract

This study presents the mechanism of underexcavation and practical design method for building rectification. Underexcavation is widely used to restore for not only historic monuments but also modern steel–concrete buildings that undergo large differential settlement. Due to the lack of systematic theoretical research and design specifications, the rectification process mainly depends on real-time monitoring. To meet the urgent need to address building tilt whether caused by design errors or by environmental changes, a plane strain numerical simulation is introduced to probe the mechanism of underexcavation for building rectification. The whole process of soil failure and deformation during underexcavation have been analysed with a series of numerical models, and a simplified analysis method has been proposed for predicting key parameters for the design of a building rectification. The simulation results of a single-hole excavation demonstrate the features of soil stress redistribution, the character of the displacement field, the modes of soil failure and the expansion characteristics of the failure zone. The results of simulations of multi-hole underexcavation show the relationship between plastic failure around the holes and global failure of the shallow foundation and indicate that hole closure is the main source of deformation during rectification. Based on the numerical simulation results combined with engineering experience, two key parameters of optimum spacing and hole diameter are obtained.

## Article Highlights

- The finite element simulation reveals the details of stress field and displacement field around the underexcavation hole, which is difficult to capture in site observation or in model test; The soil failure takes the underexcavation hole as the defect center and develops in the shape of "X", which is very different from the previous study but agrees with the laboratory tests.
- The multi-hole finite element simulation shows that the deformation caused by stress redistribution is negligible compared to the anticipated forced settlement, which indicates that the forced settlement is from the hole closure. This simulation provides a basis for derivation of key parameters of rectification design.
- According to the total vertical force balance between the bottom of the base and the horizontal plane at hole centre line, the formula for the preferred hole spacing is obtained; According to that the amount of base settlement is equal to the volume of soil excavation, the formula for the hole diameter is obtained. The two formulas can assist geotechnical engineers with the rapid design scheme for building rectification.

---

✉ Junhua Xiao, 13606412056@163.com; Jianping Sun, 15069192907@163.com; Xin Zhang, zhangxin@sdjzu.edu.cn; Qingxia Yue, yueqx@sdjzu.edu.cn | [1]School of Civil Engineering, Shandong Jianzhu University, Jinan, China. [2]Key Laboratory of Building Structural Retrofitting and Underground Space Engineering (Shandong Jianzhu University), Ministry of Education, Jinan, China.

## List of symbols

| | |
|---|---|
| $c_u$ | Undrained shear strength |
| $c$ | Cohesion |
| $\varphi$ | Internal friction angle |
| $d$ | Hole diameter |
| $E$ | Elastic modulus |
| $f_a$ | Allowable bearing capacity in foundation design |
| $K$ | Safety factor of the foundation |
| $K_0$ | Coefficient of static earth pressure |
| $l$ | Hole spacing |
| $m$ | Number of rows in the excavation section |
| $N$ | Number of holes in the excavation section |
| $n$ | Ratio of hole spacing to hole diameter |
| $p$ | Contact pressure of the shallow footing |
| $p_u$ | Ultimate bearing capacity of the foundation |
| $\gamma$ | Bulk density of soil |
| $\mu$ | Poisson ratio of soil |
| $\sigma_v'$ | Vertical effective stress at the level of underexcavation |
| $\sigma_t$ | Tensile strength |
| $\sigma_1$ | Major principal stress |
| $\sigma_2$ | Medium principal stress |
| $\sigma_3$ | Minor principal stress |
| $\sigma_\theta$ | Lode angle |

## 1 Introduction

Buildings with shallow foundations on natural soil layers inevitably undergo uneven settlement due to age, design errors, changes of the surrounding environment, or underground construction. The methods used to correct building inclination can be divided into the jacking-up method, the forced settlement method, and the combined jacking-up and forced settlement method [10, 16]. Among these methods, the forced method by soil underexcavation is often adopted.

The technique of underexcavation or soil extraction, as a non-invasive method for building rectification, was first practised in 1832 on the tower of St Chad, Wybunbury, which had been experiencing continuous settlement caused by underground salt extraction and sand or silt erosion [9]. In 1962, Terracina [18] proposed the underexcavation method to increase the stability of the Tower of Pisa and suggested drilling a series of holes with different bore lengths at the side with less subsidence. This was the first time that underexcavation was formally proposed as a rectification technology. In Mexico City, this method was successfully used for rectifying historic buildings distressed by consolidation of highly compressible soft soils and modern structures that had lost their vertical orientation

during earthquakes [13, 14]. The Tower of Pisa is the project that has been studied in the most details [1–3, 6, 7]. To successfully apply rectification without causing any irreversible damage to the fragile masonry, small-scale physical tests, simplified analysis, finite element analysis and pre-excavation tests were carried out. Some qualitative understanding was obtained on the effectiveness of soil excavation, the critical line (beyond which ground removal aggravates the tilt), the simulation of settlement history used to predict the response to underexcavation, the cavity closure time, the technology of soil extraction and simulation methods of soil cutting.

In China, soil underexcavation is used for the deviation rectification of not only ancient pagodas and historic buildings [16, 23] but also a wide range of modern reinforced concrete structures [20]. Most modern structures are based on rafts, and their superstructure stiffness is large, so underexcavation is very applicable.

Those inclined buildings above mentioned were successfully rectified to a large extent owing to on-site monitoring and dynamic rectifying operations. However, theoretical research lags far behind engineering practice. To date, little attention has been given to investigating the rectification mechanism of underexcavation in a comprehensive and refined way, and there is still no design method for underexcavation. Rojas used the formula $2c_u < \sigma_v' < (2+\pi)c_u$ to calculate the conditions under which holes close due to plastic yielding [15], which represents the critical stress state at cavity closure, but this formula cannot describe stress redistribution. Ovando-Shelley and Santoyo developed an empirical expression for the lengths of cavities at different times after underexcavation for predicting settlement with time [14], but how to design the hole spacing and diameter was not given. All these studies provided some insights on rectification mechanisms, but there is still a great need for additional information before rectification can be put into common practice.

Our research team has completed more than ten rectification projects and gained valuable engineering experience. We have learned that when conducting an excavation project, there is a critical point when back-tipping accelerates, and the preferable spacing of holes is approximately 2–3 times the hole diameter in silty clay with medium strength. To further probe the rectification mechanism, several groups of scale model tests were carried out [17, 22], and the hole deformation type under different spacings, the stress transition from hole positions to intervals and the favourable hole spacings for inclination correction were obtained qualitatively. However, the relationships among the surcharge,

surface settlement, soil stress and failure mode have not been determined. Yue et al. [21] assumed that the plastic zone expanded at hole intervals and defined the failure criterion as a certain ultimate strain; a numerical analysis suggested the value of the hole spacing corresponding to failure when holes break through the soil. Nevertheless, there are still some interesting observations in scale tests that cannot be rationally explained using such ultimate strain analysis. Furthermore, in the model test, the continuous stress variation and displacement field cannot be obtained even by means of various monitored parameters, whereas only continuous stress and displacement fields provide a clearer and more comprehensive understanding of the relationship between soil extraction and surface settlement. Meanwhile, there is still no theoretical explanation for the favourable hole spacing in tests and in practice, which are 2–3 times the hole diameter.

In this paper, we present finite element simulations to investigate general trends in the process of extracting soil for correcting building inclination. Based on the simulation conclusions, we propose a simplified method to predict the design parameters in practice. Through simulations of single-hole underexcavation, the characteristics of the displacement field around the hole, the redistribution of soil stress and the evolution of the plastic zone were examined, and some previously perplexing observations became understandable. Through simulating multi-hole underexcavation, combined with engineering experience, the main source of expected settlement for rectification was confirmed, and the relationship between the final hole collapse and the ultimate capacity state of the foundation was clarified. Finally, using a simplified analytical method, two practical formulas for the favourable spacing and the diameter of the soil extraction hole were derived for building rectification design.

In the next section, we give the soil parameters and constitutive model used in the numerical simulations. Section 3 shows the simulation of single-hole underexcavation and verifies the applicability of finite element method. Section 4 presents the results of multi-hole simulation and reveals the Mechanism of underexcavation. In Sect. 5, we derive the formulas of hole spacing and diameter. Finally, some conclusions are given in Sect. 6.
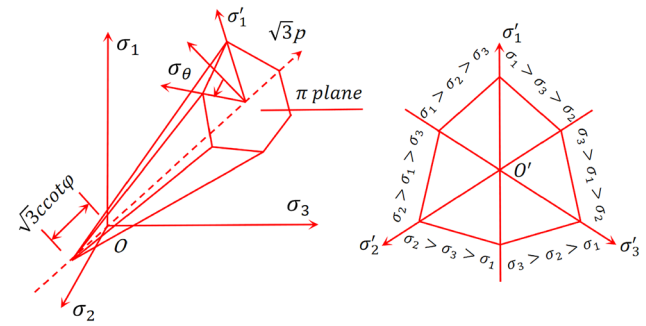


**Fig. 1** Mohr–Coulomb yield criterion in principal stress space and π plane

## 2 Soil parameters and constitutive model

### 2.1 Soil parameters

Midas GTS was used for numerical simulation and analysis of single-hole and multi-hole excavations. The horizontal excavation was simplified as a plane strain problem perpendicular to the excavation direction. The characteristics of the displacement field, stress field and plastic (failure) zone (for an ideal plastic-elastic material, the plastic zone is also the failure zone) of soil were studied under structural loading for the most common type of silty clay. The simulation process was as follows. First, the ground stress was balanced, and the displacement caused by the weight of the soil was set to zero. Then, the structure load corresponding to the proportional limit load of the foundation soil (also approaching the allowable bearing capacity of the soil) was applied, and the displacement was set to zero (corresponding to the present state of the building). The influence of foundation settlement caused by the superstructure load was eliminated on subsequent excavations. Finally, the excavation project was carried out. The soil parameters are from the "Geology Engineering Handbook" [4] and listed in Table 1.

### 2.2 Constitutive soil model

The mechanical behaviour of soil mainly depends on its constitutive model. In the simulation, the soil was taken as an ideal elastic–plastic body with no strain hardening or softening characteristics, so its yield criterion is the failure criterion [24]. The Mohr–Coulomb criterion has been widely used in geotechnical analysis due to its high accuracy and

**Table 1** Geotechnical parameters for simulations

| Soil name | $\gamma$ (kN/m$^3$) | E (MPa) | $\mu$ | $K_0$ | c (kPa) | $\varphi$ (°) | $\sigma_t$ (kPa) |
|---|---|---|---|---|---|---|---|
| Silty clay | 19.0 | 15 | 0.3 | 0.66 | 30 | 20 | 5 |

application convenience. In the principal stress space and π plane, the shape of the yield (failure) surface are shown in Fig. 1.

The Mohr–Coulomb criterion states that the ultimate shear stress on any plane is related to the normal force on that plane and the shear strength parameters of the soil. When the principal stresses satisfy $\sigma_1 > \sigma_2 > \sigma_3$, it is expressed as follows:

$$\frac{\sigma_1 - \sigma_3}{2} = \frac{\sigma_1 + \sigma_3}{2} \sin\varphi + c\cos\varphi \qquad (1)$$

## 3 Analysis of plastic zone evolution by a single-hole simulation

To investigate the whole process of plastic zone evolution as well as soil stress and displacement after underexcavation, a single-hole simulation was conducted. The hole diameter was 200 mm. A simple model was considered to make the underlying mechanism of the underexcavation easier to understand.

### 3.1 Initial stress field

In the simulation of single-hole underexcavation process, the surcharge load was 120 kPa, corresponding to the elastic load limit or the proportional load limit of the soil, beyond which shear failure would occur in the soil below a shallow foundation. This critical value of the surcharge load was determined by a series of trial simulations.

Under the surcharge load, the initial vertical stress field in the foundation subsoil is shown in Fig. 2. The %s in Fig. 2 and following Figs indicate the area percentages of bands in contour map of simulation results. The vertical stress

field around the site where the hole will be excavated is close to the base pressure. At this simulation step, the displacement field is cleared to zero. For the plane strain problem, whether the stress in the direction other than the loading direction is a medium or a minor principal stress depends on the material parameters and three-dimensional stress state [12]. In this numerical model in initial state, the medium principal stress is in the X direction, and the minor principal stress is in the third or Z direction. Taking the centre point of the base as an example, $\sigma_1 = \sigma_y = 120kPa$, $\sigma_2 = \sigma_x = 80kPa$ and $\sigma_3 = \sigma_z = 60kPa$.

### 3.2 Displacement field

Figure 3 shows the displacement field around the hole after soil extraction. The distribution of the rebound displacement is nonuniform around the hole, and the vertical rebound is much larger than the horizontal rebound. The rebound transfers from the top of the hole to the ground surface and thus causes the base to move downward. At the "arch foot" of the hole, the total displacement vector deflects. This simulated displacement is consistent with the short-term ground displacement measured during EPBM tunnelling in London clay [19]. Unlike from the measured displacement, this simulation more clearly shows the displacement features, helping to reveal the underexcavation mechanism.

### 3.3 Stress redistribution

Figure 4 shows the vertical stress redistribution and the change amount after the excavation. Apparently, compared to the initial stress of approximately 120 kPa, the vertical stress decreases significantly at the top and bottom of the hole and increases significantly on both sides
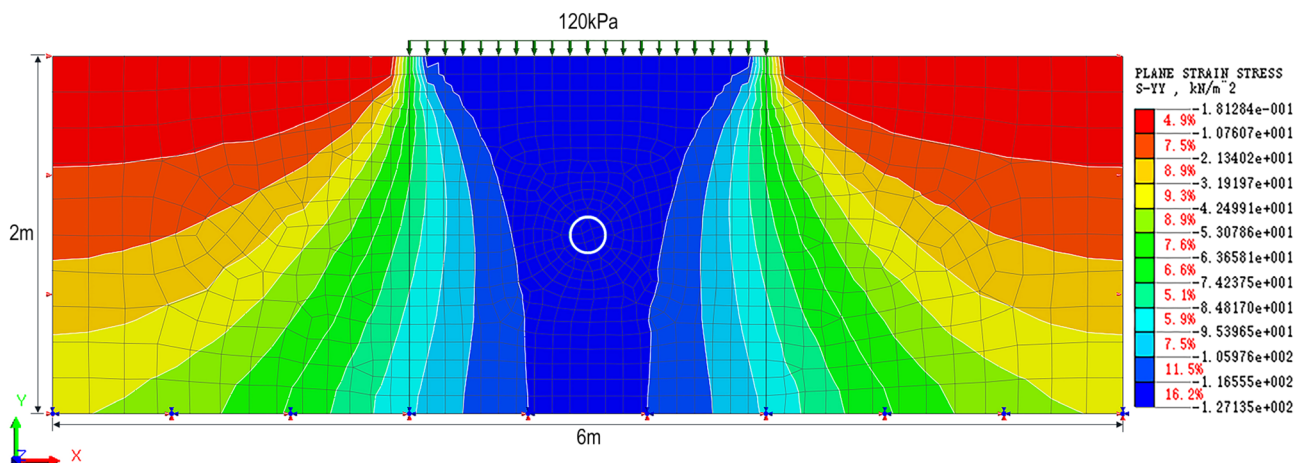


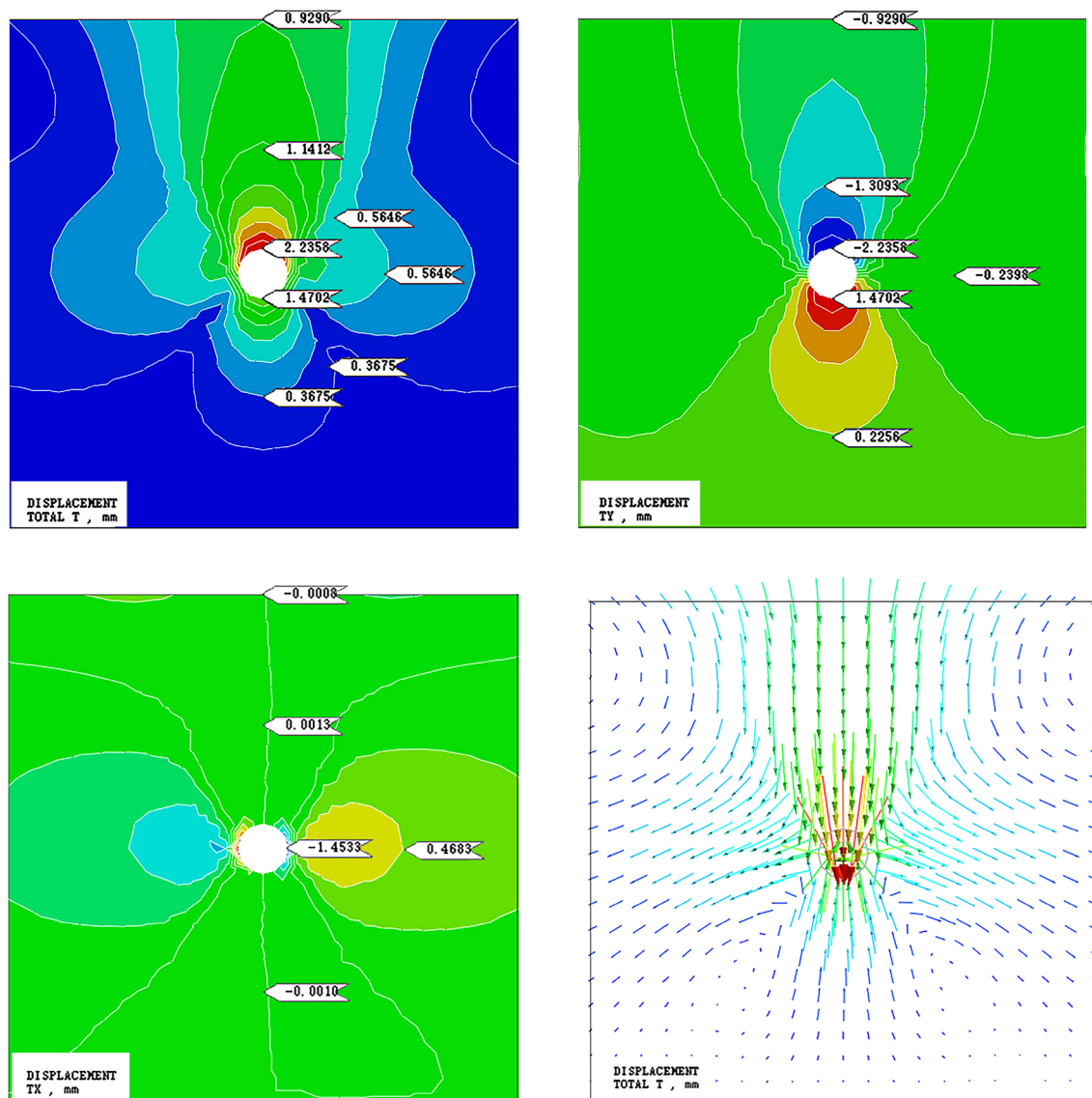**Fig. 2** Initial vertical stress field before underexcavation

**Fig. 3** Displacement field after the hole was cut

of the hole; that is, the stress around the hole transfers and flows in the body of the soil due to the soil cutting off. This means that the foundation settlement results not only from the rebound of the soil unloading but also from soil recompression, which account for various proportions of the settlement at different horizontal positions. The stress transition agrees well with our previous model tests [22]. Furthermore, this simulation provides contour maps of the additional stress on the foundation, shown in Fig. 4a, and the change in stress, shown in Fig. 4b, which more clearly present the stress transition trends.

## 3.4 Plastic zone evolution

In practice, the methods of repeatedly excavating, reaming, filling with water and applying a surcharge load are usually adopted to accelerate the plastic flow of foundation soil to promote base settlement. To clearly demonstrate the evolution of the plastic zone around the hole, an incremental load was applied to the foundation surface during the simulation. Figure 5 shows the plastic zone evolution when the load was increased stepwise from 120 to 180 kPa. Just before starting the underexcavating process, the plastic zone beside the foundation base was caused by
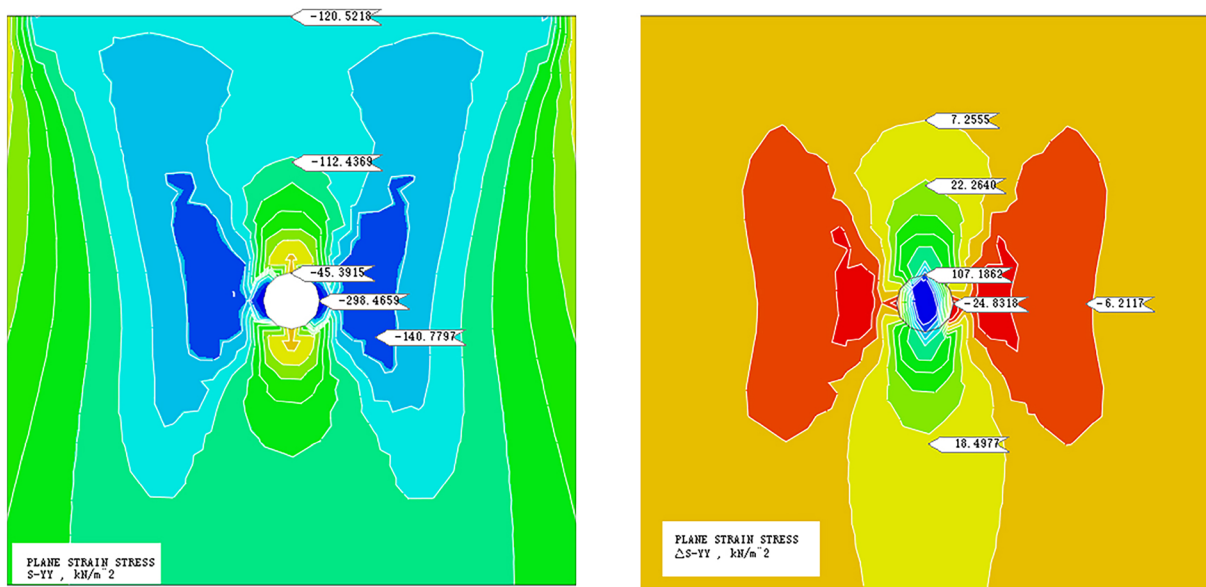
**Fig. 4** Redistribution of the vertical stress and the change amount around the hole

the initial load of 120 kPa not by excavation, so attention should be given to the change in material status in this region at the subsequent loading.

Figure 5 shows the following important indications: (a) Under the load from upper structure, the subgrade soil takes the hole as a "defect" centre and develops a plastic zone with an X-shape; the plastic zone strip is at an angle of approximately 45° + φ/2 relative to the large principal plane (completely consistent with the soil shear strength theory). (b) As the upper load increases, the plastic zone expands and gradually deviates from the original shear failure line of 45° + φ/2. The plastic zone is probably attracted by the plastic zone at the ground surface and finally connects with it when the load reaches 180 kPa. (c) Under the maximum surcharge load, tensile failure occurs near the ground surface beside the foundation base. All these signs imply that although the goal of soil excavation is to promote settlement of the side of the target building with lower subsidence, the process of soil excavation is always related to the safety margin of the load bearing capacity of the soil; with the advancement of the correction to the inclination, the local shear failure gradually approaches the global shear failure of the foundation.

### 3.5 Explanation of the previous scale test observations

Our team carried out detailed scale model tests on silty clay to study the hole failure mode and soil stress transition characteristics for different excavation spacings and upper load conditions [17, 22]. The model box is shown in

Fig. 6a. The volume of the model box is 3 m × 3 m × 2.5 m and the box is made of steel plate. On the side of the soil cutting surface the steel plate is detachable (see Fig. 6a). The soil used in the test was remolded silty clay, which had been compacted manually in layers in the model box. Before the test started, the soil was sampled and tested to obtain the values of the most important geotechnical parameters: water content (16.5%), bulk density (1.85 g/ cm$^3$), cohesion (16 kPa) and internal angle of friction (20 deg). A concrete slab of 2 m × 1.5 m was placed on the soil top surface, and the load was applied by laying concrete blocks.

The hole diameter was 150 mm, which was limited by the width of the detachable steel plate. The tests were carried out under three working conditions: case 1 was under the pressure of 66.6 kPa with the hole spacing of 4 d; case 2 was under the pressure of 66.6 kPa with the hole spacing of 3 d; and case 3 was under the pressure of 66.6 kPa with the hole spacing of 2 d, and then increasing the pressure by two increments to 76.6 kPa and 86.6 kPa successively. The maximum load was limited to avoid damage of the surrounding steel beams or joints of the model box.

The stress redistribution in the soil after hole excavation was examined. The rotation of the "superstructure" was observed by measuring the concrete block vertical edge. The soil deformation was not measured directly, but the deformation phenomena were recorded by photos. The results of the model tests were mainly published in the Master's thesis written by Sun entitled "Experimental study on failure mechanism of under excavation method for building rectification" in Chinese (Sun H, 2019). The soil
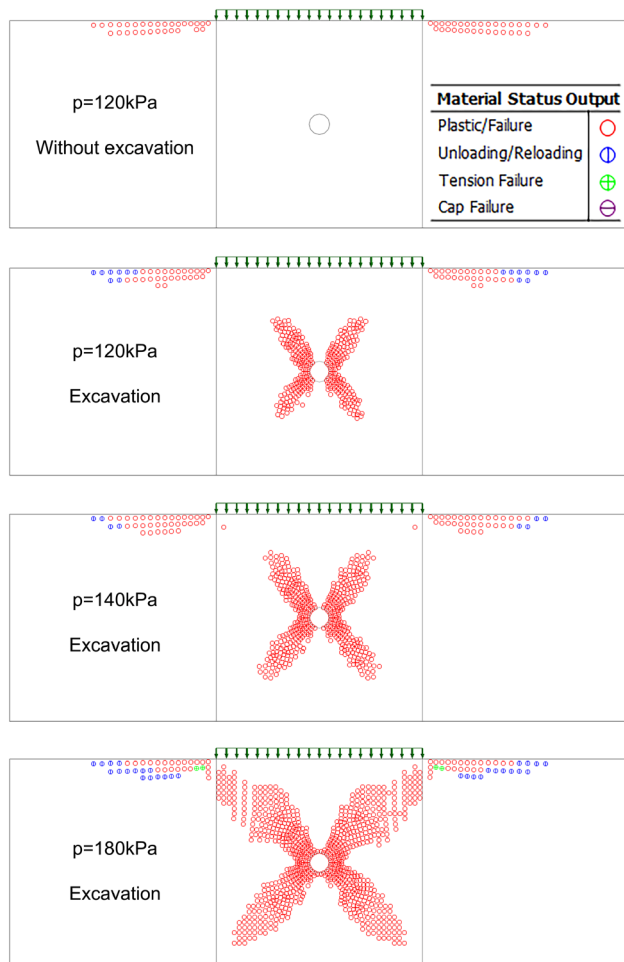
**Fig. 5** Evolution of the plastic zone with the increase of surcharge load

deformation phenomena and the explanation were published in [22]. Nevertheless, there are still some strange observations not being explained such as ridge lines in soil holes.

The stress transfer trend obtained from the point measurements in the scale tests is completely consistent with the above simulation results. The trend is stress transferring from the hole top to the hole side. Here, utilising the continuous and more accurate simulation results, we focus on the test observations and provide explanations, especially for the perplexing observations.

The characteristic deformation during the test can be summarized in three stages: (1) When the surcharge load was low, the visible deformation first appeared in the lower half of the hole, including the symmetrical "ridge line" on the sidewall shown in Fig. 6b and the heave with some loose soil particles at the bottom of the hole. (2) With the increase in surcharge load or the decrease in hole spacing, the deformation of the lower half of the hole became more

obvious, while a small amount of soil particles started falling down or diagonally from the top of the hole, as shown in Fig. 6c and (3) As the load continued to increase or the hole spacing was further decreased, there was minor collapse of the hole sidewall, the falling particles of soil at the top of the hole became more severe (heave at the bottom of the hole could not be seen due to the layer of fallen soil), and the entire hole started to collapse, as shown in Fig. 6d. Meanwhile, cracks developed on the ground surface as shown in Fig. 6e.

Comparing the deformation phenomena with the numerical simulation results, we can obtain the following understandings:

(a)  With the increase in the surcharge load, the soil around the holes deforms and evolves dynamically, presenting various features of deformation and strength failure modes at different stages.

(b)  The soil behaviour displayed in the tests can be explained using simulation results. The symmetrical "ridge line" on the hole sidewall is actually the result of displacement deflection or squeeze-like collisions (refer to Fig. 3); the roof collapse and bottom heave are rebound deformations caused by unloading as a result of the underexcavation process; the soil falling diagonally from a location above the hole is actually due to soil shear failure (refer to Fig. 5); and the surface cracks are an indication of tensile failure caused by settlement (also refer to Fig. 5).

(c)  In the simulation, the rebound deformation at the top of the hole was greater than that at the bottom of the hole. In contrast, the hole bottom heave observed in the scale test was more obvious than rebound deformation of the hole top, probably because there was a soil arching effect at the top of the hole, and the soil is not an ideal elastic-plastic body.

(d)  There are several actual failure modes of the bulk soil in the scale test. In practice, engineering includes not only strength failure modes such as shear failure and tensile failure but also deformation failure modes such as rebound heave, rebound tension, and squeeze-like collisions. Among these failure modes, the strength failure criterion is included in the Mohr-Coulomb constitutive model used in the numerical simulation, but the other modes are not included due to the complexity of the mechanical behaviour of the soil and the limitation of the constitutive model. In a previous scale test, Yue and Zhang [22] defined three failure modes, i.e., a vertical irregular ellipse, a horizontal irregular ellipse, and an irregular circle, at different surrounding stresses. This definition is based on the combined deformation phenomena, not on the principles of soil mechanics. The simulated shear

**Fig. 6** Model box and typical observations, **a** Model box, **b** Ridge line, **c** Shear failure with an X-shape and particles falling from the roof, **d** The hole approaching collapse, **e** Cracks on the ground surface
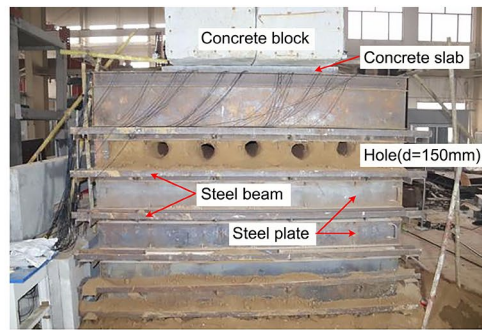


(a) Model box



(b) Ridge line

(c) Shear failure with an X-shape and particles falling from the roof



(d) The hole approaching collapse

(e) Cracks on the ground surface

failure is completely consistent with the principles of soil mechanics and verified by scale test observations.

(e) When the soil strips between the holes collapse, the behaviour of the soil cannot be observed due to hole closure; meanwhile, the finite element method cannot further simulate the behaviour of the collapsed soil because this method is not suitable for a discontinuous material.

In summary, the numerical simulation verifies the vertical stress transition obtained from the previous scale test and gives a reasonable and highly accurate explanation for the previously observed test phenomena (except for that of the cracked soil after hole collapse); more importantly,

it shows the sequence of continuous stress transitions, revealing the plastic zone expansion behaviour. This comparison between the simulation and test results indicates that the constitutive model is applicable, the simulation method is feasible and the simulation results are credible.

## 4 Evaluation of the rectification mechanism by a multi-hole simulation

In engineering practice, multi-hole excavation is always used for inclination correction. To better investigate the mechanism of inclination correction by soil excavation, a numerical model of multi-hole excavation was

established. The model size was 4 m × 12 m, and the foundation width was 4 m at the site where a surcharge load was applied. The distance of the hole from the bottom of the foundation was 1.0 m, and the hole diameter "d" was 200 mm. Two cases were studied at 4 d and 2 d spacing of adjacent holes.

The elastic load limit of the model foundation was determined to be 120 kPa by trial finite element calculations. Under this load, several elements below the foundation base underwent plastic failure, whereas in the single-hole simulation, no elements below the foundation base underwent shear failure at the same load. This is because the bearing capacity of a certain kind of soil with specific shear strength parameters is not a constant value but varies with the footing width, calculation method, and constitutive model in a finite element analysis [5, 8, 11]. In foundation design, the allowable bearing capacity is often taken as equal to or slightly larger than the elastic load limit, so this value basically represents the service state of the building before excavation. The values of the soil parameters were taken to be the same as those of the single-hole model.

## 4.1 Displacement analysis

The total displacement of soil excavation at 4 d and 2 d spacing is shown in Fig. 7, the comparison of the vertical displacement is shown in Fig. 8, and the comparison of the vertical displacement at different horizontal levels is shown in Fig. 9.

Figure 7 shows that the total displacement caused by excavation mainly occurs between the foundation base plane and the underexcavation plane. This indicates that the influence of the inclination correction of a building on the surrounding environment is very small.

Figure 8 shows that in terms of vertical displacement, the soil in the roof of the hole rebounds downward, while the soil at the bottom of the hole rebounds upward. The vertical displacement of the soil in the perpendicular direction above or beneath the hole is mainly caused by unloading rebound, whereas those of the soil between the holes are mainly caused by soil re-compression due to stress transitions, and the re-compression displacements are much smaller than the rebounding displacements.

Figure 9 shows the vertical displacement values on different horizontal planes marked in Fig. 8 for two cases of hole spacing. It can be seen from Fig. 9: (a) With decreasing hole spacing, the vertical displacement of the foundation, i.e., the ground surface, increases from
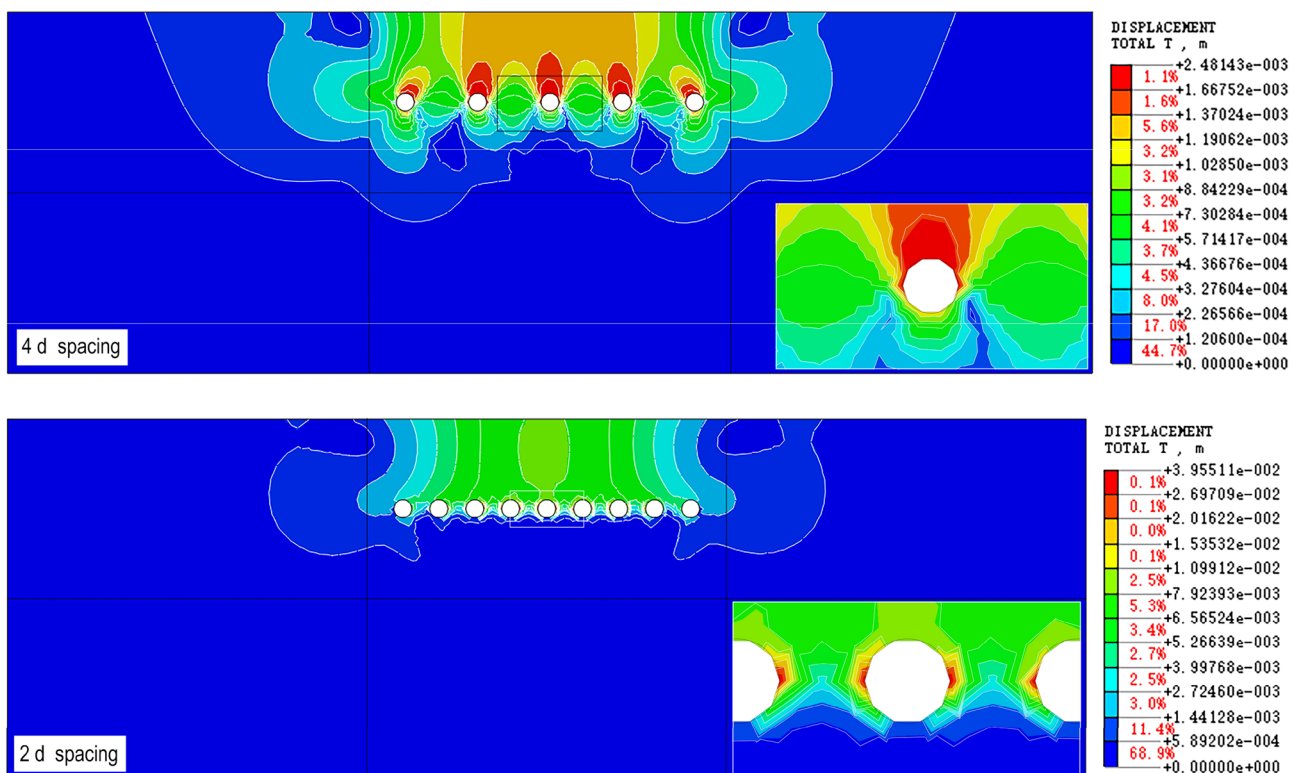


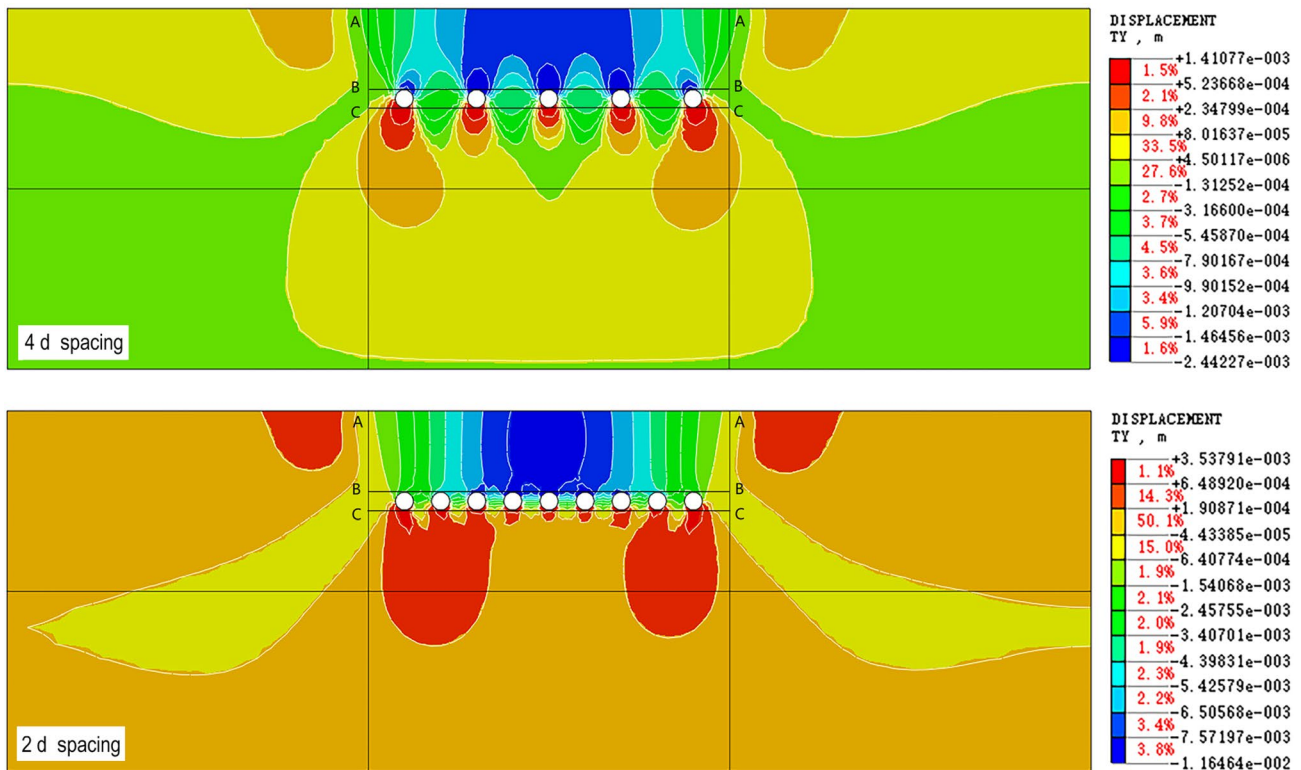**Fig. 7** Total displacement of soil extraction openings at 4 d and 2 d spacing

**Fig. 8** Comparison of the vertical displacements at 4 d and 2 d spacing
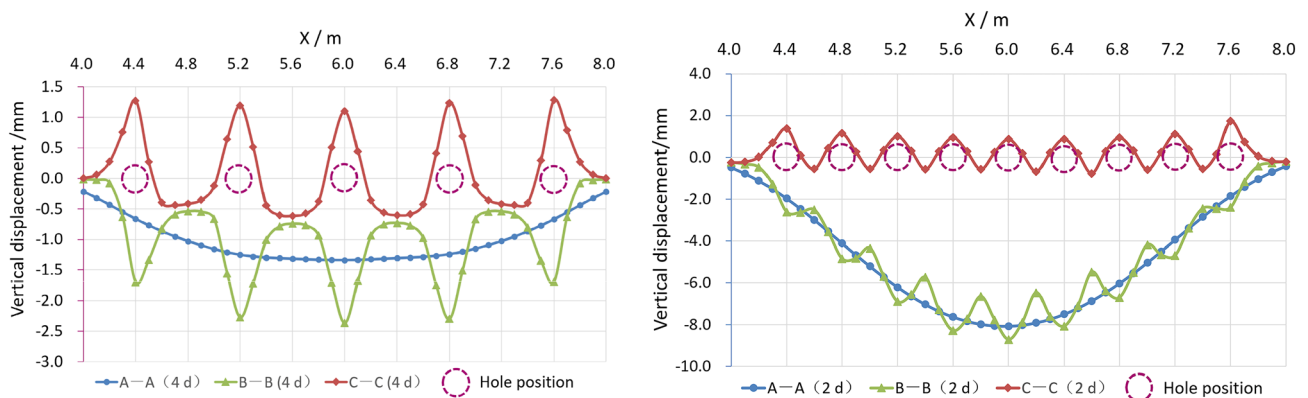


**Fig. 9** Comparison of vertical displacements at different horizontal levels

1.3 mm of the maximum settlement at 4 d hole spacing to 8.1 mm at 2 d hole spacing. (b) The displacement difference between the roof point and the bottom point increases as the hole spacing decreases, from 3.5 mm at 4 d spacing to 9.5 mm at 2 d spacing, reflecting the degree that the hole flattened; from the perspective of deformation, this can explain why the soil holes show different failure modes defined by Yue and Zhang [22]. (c) At the hole intervals, the soil strip is re-compressed from 0.1 mm of compression at 4 d spacing to 5.8 mm

at 2 d spacing, reflecting the transfer of more stress at the smaller hole spacing, which is compatible with the ultimate strain analysis by Yue et al. [21].

It is important to note that the simulated vertical displacement at the ground surface is in the order of millimeters for the arrangement of holes that is equivalent to engineering situations. This is far less than the settlement observed in practice during building rectification, which is in the order of centimeters.
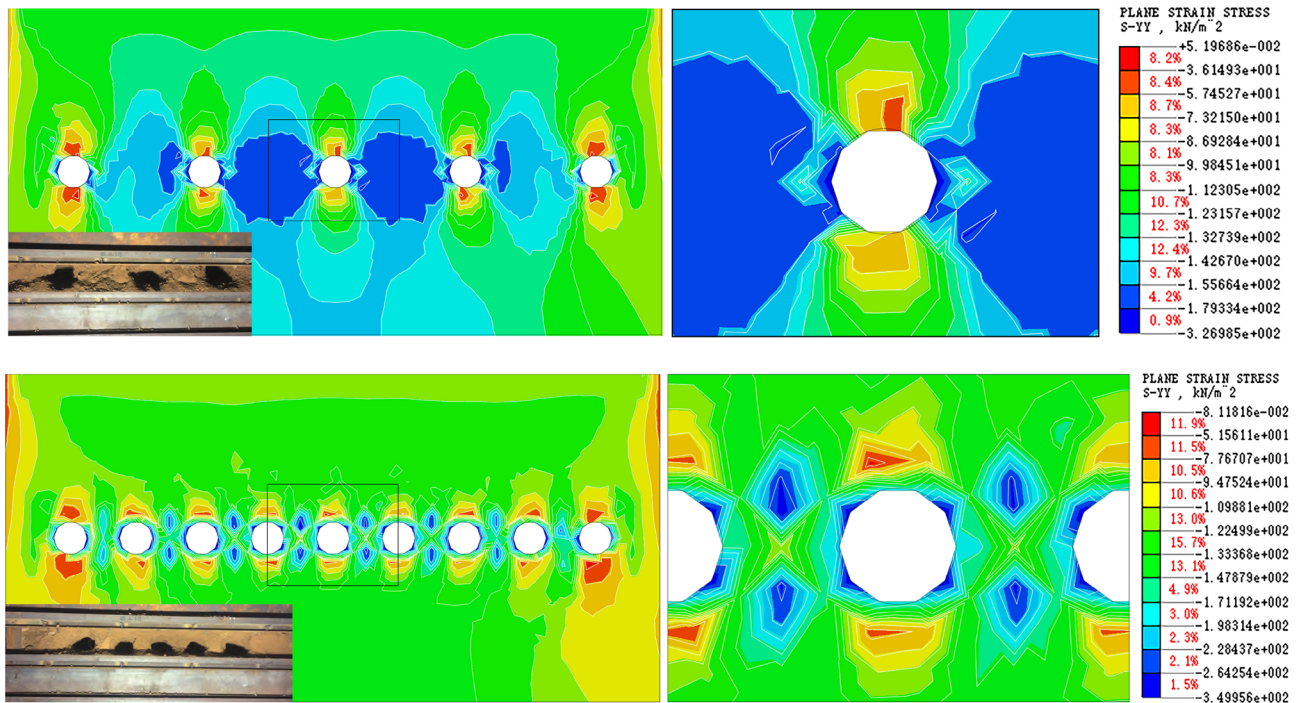
**Fig. 10** Vertical stress comparison at 4 d and 2 d spacing

## 4.2 Stress analysis

The comparison of vertical stress redistribution at two different spacings is shown in Fig. 10. In the vicinity of the excavation hole, the vertical stress redistributes markedly, forming areas of increasing and decreasing stress between the holes and above and below the holes, respectively. When the hole spacing is 2 d, the soil strip between the holes resembles an X-shape low stress area surrounded by a high stress area, and the high stress reaches or even exceeds two times the elastic load limit of the foundation, i.e., 240 kPa. This value implies that the soil strip has been sheared or at least approaches failure. This conclusion is also supported in principle by other researchers [14, 15]: "Classical plasticity provides simple solutions for checking whether the soil around a cavity will yield and close the holes left by underexcavation, depending on the soil's undrained strength and the effective stresses acting on it at a given depth. The conditions under which the boreholes will close due to plastic yielding of the soil are $2c_u < \sigma'_v < (2+\pi)c_u$".

Soil strip failure or hole collapse is also suggested by the previous scale test (see Fig. 6), as shown in the embedded photos in Fig. 10. Under the condition that the surcharge load was less than the elastic load limit of the soil, at 4 d spacing, the soil strip was partly crushed, but the hole was still basically intact; at 2 d spacing, the
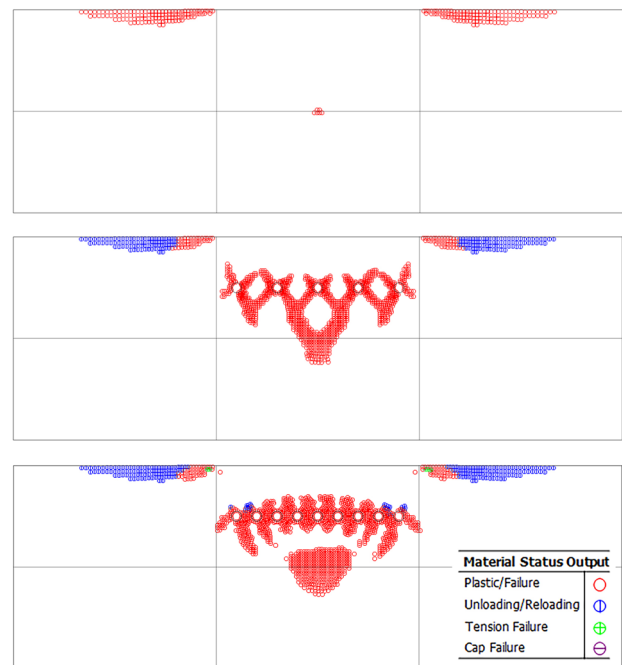


**Fig. 11** Plastic zone evolution of the multi-hole excavation

soil strip was crushed more severely, and the lower part of the hole almost disappeared.

Figure 11 shows the evolution of the plastic zone under the condition of multi-hole excavation. Before excavation,

a surcharge load of 120 kPa was applied, and the plastic (failure) zone under the "base" just started to appear, which indicated that the allowable capacity of the foundation soil was near this value. On both sides of the loaded surface, two symmetrical plastic zones emerged, mainly because the loading was at the ground surface, i.e., the buried depth of the "base" was zero. Therefore, this plastic zone could be ignored in the analysis. After excavating at 4 d spacing, the plastic zone formed and was centred on the hole, and then it expanded; a deeper plastic zone formed below the hole line, and there was an indication of unloading due to soil settlement at the surface beside the loaded area. When the soil extraction proceeded to 2 d spacing, the plastic zones around the holes expanded, became connected and seemed to be attracted by the deeper plastic zone. Meanwhile, near the ground surface, tensile fracture occurred. All signs implied that the foundation safety was approaching the ultimate state of failure.

### 4.3 Mechanism of underexcavation for inclination correction

Through numerical simulation analysis, combined with engineering experience and model tests, the rectification mechanism by soil underexcavation is summarized as follows: soil excavation with small holes causes stress redistribution in the soil, and the soil undergoes rebound deformation and re-compression deformation. This rebounding and re-compression leads to elastic settlement at the ground surface; the X-shape failure-zone develops around the hole, and in addition to this strength failure mode, large strain failure modes, such as tension failure and squeeze collision failure, develop in practice, although the strain failure mode cannot be reflected in the Mohr–Coulomb constitutive model; with the decrease in hole spacing or the increase in surcharge load, the plastic zone expands, and more vertical stress is transferred to the soil strips between holes; when the soil between holes reaches the ultimate capacity state, the soil strips collapse, and the holes tend to close (in practice, by filling with water or collapsing under a load surcharge).

As far as the source of expected settlement at the surface for inclination correction is concerned, the elastic deformation before hole collapse is very small, only of the order of millimeters in the simulated case; For an ideal elastic plastic body, even if large plastic zones develop, as long as the soil does not have the characteristics of shear shrinkage, the plastic zone will not cause further settlement of the base. However, the expansion of the plastic zone helps to transfer more stress to the surroundings, which increases the stress on the soil strip and promotes its collapse. After the hole collapses, the finite element method cannot continue to simulate the mechanical behaviour of the soil. The hole cavity is filled with collapsed soil; thus, hole collapse deformation is the main source of the desired settlement for building inclination correction. This conclusion is also supported by Ovando-Sheelley and Santoyo [14], who wrote that the magnitudes of the settlements observed in practice "do not account for volume changes in the soil mass around the underexcavated zone, produced by increases in compressibility as a consequence of re-moulding of the soils around the underexcavation cavities and by effective stress changes within the soil mass".

## 5 Design formula by simplified analysis

### 5.1 Favourable hole spacing

The favourable hole spacing is the minimum spacing limit. At this spacing, the vertical stress in the soil strip between holes is greatly increased and approaches the ultimate capacity of the soil. Under such critical conditions, the soil strip tends to collapse, so the optimum spacing is most effective and favourable for building rectification.

The simplified analysis is based on a certain underexcavation section perpendicular to the cutting direction shown in Fig. 12, assuming that the length along the excavation direction is 1 m. The hole is generally set at 1.0–2.0 m below the footings in engineering projects, so the dispersion of the base pressure to the hole position can be ignored. In the original building design, the base pressure $p$ is often taken as the allowable bearing capacity $f_a$ of the bearing stratum. This means that under the building's service condition $p \approx f_a = p_u/K$.

As shown in the analysis diagram in Fig. 12, the diameter of the hole is $d$, the hole spacing is $l$, and there are $N$ holes at the underexcavation section. The effective area of
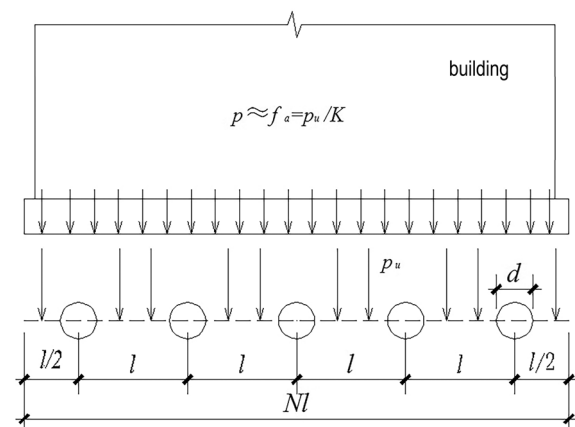


**Fig. 12** Analysis diagram for optimum spacing of excavation hole

the base pressure is the width of the digging section, $Nl$. Due to soil cutting, the bearing area at the hole centre line level is decreased to $N(l − d)$.

When the soil strip is close to the crushing state, the vertical stress at the strip approaches the ultimate bearing capacity. Because the total force at the base level is equal to that at the hole centre line level, we can establish the force balance formula as:

$$Nlp = N(l − d)p_u \tag{2}$$

Substituting $p \approx f_a = p_u/K$ to it, we obtain

$$Nlp_u/K = N(l − d)p_u \tag{3}$$

Therefore, the optimum hole spacing is obtained:

$$l = \frac{K}{K − 1}d = nd \tag{4}$$

where $n = \frac{K}{K−1}$, $K$ is the safety factor of the bearing capacity of the foundation during the building service life, $K = p_u/p$.

Considering that the foundation safety margin of inclined buildings is less than that of those buildings in good conditions, we can take $K$ as 1.5–2.0; thus, the corresponding favourable hole spacing is (2–3) d, which is supported by the previous model test results and engineering experience.

## 5.2 Diameter of the hole

Collapse deformation is the main source of expected settlement for inclination correction. Taking a certain cross section for analysis and assuming that the proposed settlement is s, then the hole spacing is $l = nd$, and the design includes m-rows of soil extraction holes. The analysis diagram is shown in Fig. 13. Under the condition that the volume of settlement at the basement level is equal to the volume of excavation soil, the following formula is obtained:
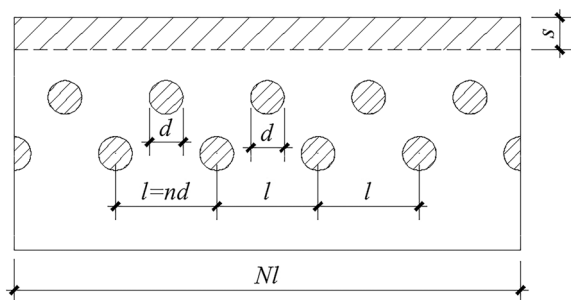


**Fig. 13** Analysis diagram for diameter of excavation hole

$$sNl = mN\frac{\pi d^2}{4} \tag{5}$$

i.e.,

$$sNnd = mN\frac{\pi d^2}{4} \tag{6}$$

Thus, the diameter of hole is obtained:

$$d = \frac{4ns}{m\pi} \tag{7}$$

Additionally, the surface settlement can be predicted by the following formula:

$$s = \frac{m\pi d}{4n} \tag{8}$$

The above two formulas of favourable spacing and of diameter of hole provide a theoretical guidance for building rectification design; nevertheless, on-site construction management and real-time monitoring are still very important. The design step and the formula verification in case studies will be discussed in another paper.

## 6 Conclusions

Unlike the previous case studies described in [2, 9, 14, 20], the present study was based on prior engineering experience and scale model tests but focused on rectifying mechanism and its practical application. Systematic research on the underexcavation process for building rectification was first conducted by plane strain numerical simulations on single-hole and multi-hole soil extractions, and then formulas for key parameters used in the design of rectification procedures were established by a simplified analysis. Some conclusions and remarks are as follows:

(1) The simulation of a *single hole excavation* shows that soil rebound and re-compression in the hole sidewall cause settlement of soil at the ground surface or foundation base. The soil stress redistributes around the hole, the stress at the top and bottom of the hole decreases, and the stress at both sides of the hole increases. With the increase in excavation area or loading increment after excavation, the plastic zone develops around the hole and extends to the ground in an X shape with the hole as its centre. Through comparisons with the observations from the previous model test, the feasibility and validity of the finite element simulation are confirmed, and typical

deformation phenomena in model tests are fully and reasonably explained.

(2) The results of the simulation of *multi-hole excavations* indicate that the development of vertical displacement after excavation is mainly confined to the foundation soil above the excavation holes, and the vertical settlement caused by excavation is an order of magnitude less than the required and observed settlements of buildings rectified in practice. With the increase of the soil extraction area, the X-shape plastic zone along the hole expands continuously. When the hole spacing is 2 d, the X-shape plastic zone is transversely connected, and the X-shape low stress zone surrounded by a high stress zone appears in the soil strip between the holes. At the same time, the whole foundation is close to the state of ultimate capacity. According to the simulation results together with the previous test results and engineering experience, the mechanism of underexcavation for building rectification is determined: excavation causes stress redistribution in the foundation soil, and with the increase of the excavation area or the surcharge load, the foundation soil around the hole evolves from elastic-plastic deformation to collapse. The filling of the cavity with collapsed soil is the main source of expected foundation settlement for building rectification.

(3) On the basis of the mechanism of underexcavation for correcting inclination, the formula for the preferred hole spacing, $l = \frac{K}{K-1}d = nd$, is obtained according to the total vertical force balance between the bottom of the base and the horizontal plane at hole centre line when the soil strip reaches the state of ultimate capacity. According to that the amount of base settlement is equal to the volume of soil excavation at each meter along excavation hole, the formula for the hole diameter, $d = \frac{4ns}{m\pi}$, is obtained. These formulas link the strength and deformation of the bulk soil, the control limit on safety and the control target for inclination correction. The two formulas can assist geotechnical engineers with the rapid design of schemes for building rectification.

Underexcavation for building rectification is a high-risk technology. There are still many problems to be further studied, such as how the base pressure redistributes due to structure load eccentricity, how to arrange soil cutting holes in the whole base plan, and how to better understand the remoulding and time effects produced by soil extraction. The finite element method cannot tackle the simulation of discontinuous collapsed soil. The two practical design formulas provide diagrams for the control of the effectiveness and safety of inclination correction. For each specific project, comprehensive analysis, thoughtful design, dynamic on-site manoeuvring and close monitoring are still absolutely necessary.

**Data availability** Data will be made available on reasonable request.

## Declarations

**Conflict of interests** The authors have no relevant financial or non-financial interests to disclose.

**Ethical approval** This article does not contain any studies with human participants or animals performed by any of the authors.

## References

1. Burland JB, Jamiolkowski MB, Viggiani C (2009) Leaning tower of Pisa: behaviour after stabilization operations. ISSMGE Int J Geoengin Case Hist 1:156–169
2. Burland JB, Jamiolkowski M, Viggiani C (2015) Underexcavating the tower of Pisa: back to the future. Geotech Eng J SEAGS AGS-SEA 46:126–135
3. Burland JB, Potts DM (1994) Development and application of a numerical model for the leaning tower of Pisa. IS Pre-Fail Deform Charact Geomater 2:715–738
4. Chang SB, Luo SM (2007) Geology engineering handbook. China Architecture and Building Press, Beijing, China (**in Chinese**)
5. Chwała M (2019) Undrained bearing capacity of spatially random soil for rectangular footings. Soils Found 59:1508–1521. https://doi.org/10.1016/j.sandf.2019.07.005
6. Federico F, Ferlisi S (1999) Time evolution of stability of leaning towers. Trans Built Environ 39:485–495

7. Federico F, Ferlisi S (1999) Effects of a counterweight on tilt evolution of leaning towers. Trans Built Environ 39:495–506

8. Gourvenec S, Randolph M, Kingsnorth O (2006) Undrained bearing capacity of square and rectangular footings. Int J Geomech 6:147–157. https://doi.org/10.1061/(ASCE)1532-3641(2006)6:3(147)

9. Johnston G, Burland JB (2001) An early example of the use of under excavation to stabilize the tower of ST Chad, Wybunbury in 1832. https://www.researchgate.net/publication/237678149. Accessed 3 Sep 2021

10. Kijanka M, Kowalska M (2017) Inclined buildings-some reasons and solutions. IOP Conf Ser Mater Sci Eng 245:022052. https://doi.org/10.1088/1757-899X/245/2/022052

11. Kasama K, Whittle AJ (2011) Bearing capacity of spatially random cohesive soil using numerical limit analyses. J Geotech Geoenviron Eng 137:989–996. https://doi.org/10.1061/(ASCE)GT.1943-5606.0000531

12. Lu D, Yao YP, Zhou A (2006) Relationship between principal stresses of soil mass under plane strain condition. Chin J Rock Mech Eng 25:2320–2326 (**in Chinese**)

13. Moghaddam RB, Yzquierdo LC, Jayawickrama PW (2015) Use of sub-excavation method for foundation remediation: a case study. In: International conference on geotechnical engineering (ICGE-2015). ICGE, Colombo, Sri Lanka

14. Ovando-Shelley E, Santoyo E (2001) Underexcavation for leveling buildings in Mexico City: case of the Metropolitan Cathedral and the Sagrario Church. J Archit Eng 7:61–70. https://doi.org/10.1061/(ASCE)1076-0431(2001)7:3(61)

15. Rojas E, Romo MP (1994) Comportamiento de una probeta cilíndrica con perforación central y su aplicación al procedimiento de subexcavación (Behavior of a cylindrical specimen with a central borehole and its application to the underexcavation procedure). Internal Report Inst de Ingeniería, Universidad Nacional Autónoma de México, México City (**in Spanish**)

16. Shen ZL, Wang Z (2011) Rectification and reinforcement technology of ancient pagoda. Beijing, China (in Chinese)

17. Sun H (2019) Experimental study on failure mechanism of under excavation method for building rectification. MSc Thesis, Shandong Jianzhu University, Jinan, China (in Chinese)

18. Terracina F (1962) Foundation of the leaning tower of Pisa. Geotechnique 12:336–339. https://doi.org/10.1680/geot.1962.12.4.336

19. Wan MSP, Standing JR, Potts DM, Burland JB (2017) Measured short-term ground surface response to EPBM tunnelling in London Clay. Géotechnique 67:420–445. https://doi.org/10.1680/jgeot.16.P.099

20. Xu XD, Jia LD, Sun JP, Zhao KZ, Zhang X, Li SM (1999) Design and practice of rectifying leaning building by digging-out soil and filling-in with water method. J Build Struct 20:59–65 (**in Chinese**)

21. Yue QX, Xu WN, Zhang X (2020) Simulation of rectification method of leaning building based on ultimate strain and engineering applications. https://doi.org/10.14006/j.jzjgxb.2020.0448 (in Chinese)

22. Yue QX, Zhang X (2020) Experimental study on the stress distribution and failure mode of the holes for under excavation in building rectification. Geo Congr 316:269–278. https://doi.org/10.1061/9780784482797.026

23. Zhou M, Su XL, Lei JS, Fang SJ (2020) Foundation reinforcement and deviation rectification of the leaning pagoda of Dinglin temple, China. Proc Inst Civ Eng Geotech Eng 173:473–484

24. Zhang XY, Yan SW (2004) Fundamentals of geotechnics plasticity. Tianjin University Press, Tianjin, China (**in Chinese**)